IMM algorithm for tracking targets that maneuver through coordinated turns

G. A. Watson and W. D. Blair

Weapons Control Division
Naval Surface Warfare Center
Dahlgren Division
Dahlgren, Virginia 22448–5000

Abstract

The interacting multiple model (IMM) algorithm uses multiple models that interact through state mixing to track a target maneuvering through an arbitrary trajectory. However, when a target maneuvers through a coordinated turn, the acceleration vector of the target changes magnitude and direction, and the maneuvering target models commonly used in the IMM (e.g. constant acceleration) can exhibit considerable model error. To address this problem an IMM algorithm that includes a constant velocity model, a constant speed model with the kinematic constraint for constant speed targets, and the exponentially increasing acceleration (EIA) model for maneuver response is proposed. The constant speed model utilizes a turning rate in the state transition matrix to achieve constant speed prediction. The turning rate is calculated from the velocity and acceleration estimates of the constant speed model. The kinematic constraint for constant speed targets is utilized as a pseudomeasurement in the filtering process with the constant speed model. Simulation results that demonstrate the benefits of the EIA model and the kinematic constraint to the IMM algorithm are given. The tracking performance of the proposed IMM algorithm is compared with that of an IMM algorithm utilizing constant velocity and constant turn rate models.

1. Introduction

One of the more difficult targets to track is an aircraft flying at high speeds and performing coordinated-turn maneuvers. The interacting multiple model (IMM) algorithm can be used for tracking such targets [1,2]. The results of previous investigations indicate that the IMM algorithm is the superior technique for tracking maneuvering targets when the computational requirements of the technique are considered [2,3,4]. The IMM algorithm consists of a filter for each model, a model probability evaluator, a state estimate mixer at the input of the filters, and a state estimate combiner at the output of the filters. The IMM algorithm uses multiple models that interact through state mixing to track a target maneuvering through an arbitrary trajectory. The state estimates are mixed according to their model probabilities and the model switching probabilities that are governed by an underlying Markov chain.

While the IMM algorithm is an excellent algorithm for tracking maneuvering targets, the maneuvering target models commonly used in the IMM (e.g. constant acceleration) can exhibit considerable model error during a coordinated-turn maneuver because the acceleration vector of the target is time varying. This modeling error can be reduced significantly through the use of a constant speed motion model with the kinematic constraint for constant speed targets. The constant speed model includes position, velocity, and acceleration as the elements of the state vector. A scalar turning rate is utilized in the state transition matrix to achieve a constant speed prediction (i.e. time update). The turning rate is computed as the magnitude of the acceleration divided by the target speed. Since this model can be used to track three dimensional target motion, it is called the 3D turning rate (3DTR) model. The kinematic constraint for constant speed targets the can be utilized as a pseudomeasurement in the filtering process as in [5] with the constant speed model. The kinematic constraint is $A \cdot V = 0$, where A is the acceleration vector and V is the velocity vector. Applying the kinematic constraint after a measurement update prepares the state estimates for the constant speed prediction. The 3DTR model that includes the kinematic constraint is called the 3DTRKC model.

Another issue with the IMM algorithm is its response at the beginning of a maneuver. For example, if a constant acceleration (CA) model is being used for maneuver response, immediately before the maneuver the CA filter will have an acceleration estimate near zero, and immediately after the maneuver that acceleration estimate must transition to the current acceleration. In order to improve this maneuver response, the exponentially increasing acceleration (EIA) model is included in the IMM algorithm. In the EIA model, the acceleration is modeled as an

0-8194-0863-8/92/$4.00

exponentially-correlated time sequence with a positive correlation coefficient to produce a state model that has a pole outside the unit circle. Thus, during prediction, the acceleration estimate at time $k-1$ is multiplied by a scalar greater than one to achieve the predicted acceleration at time k. Since the magnitude of the acceleration must increase at the beginning of a maneuver, the EIA model can improve the response of the IMM algorithm.

An IMM algorithm that incorporates a constant velocity (CV) model, an EIA model, and a 3DTRKC model is proposed for tracking targets that maneuver through coordinated turns. The tracking performance of the proposed IMM algorithm is compared with that of an IMM algorithm utilizing the constant turning rate model proposed in [6]. In that constant turning rate model, the target maneuvers are modeled as constant speed turns in a horizontal plane, and the turning rate of the target is estimated as part of the state. This model is referred to as the turning rate estimator (TRE) model.

The paper is organized as follows. Section 2 presents some background material on the kinematic constraint for constant speed targets, the EIA and TRE models, and the IMM algorithm. In Section 3, the proposed IMM algorithm is presented along with some simulation results that demonstate the benefits of the EIA model, the kinematic constraint for constant speed targets, and the 3DTR model to the IMM algorithm. Simulation results comparing the proposed IMM algorithm with the one utilizing the TRE model are given in Section 4. Concluding remarks are given in Section 5.

2. Background

The discrete-time model for a dynamical system is given by

$$X_k = F_{k-1}X_{k-1} + G_{k-1}w_{k-1} \tag{2.1}$$
$$Z_k = H_kX_k + v_k \tag{2.2}$$

where w_k is an $m \times 1$ process noise vector with $w_k \sim N(0, Q_k)$, v_k is a $p \times 1$ measurement error vector with $v_k \sim N(0, R_k)$, X_k is an $n \times 1$ state vector, and Z_k is a $p \times 1$ measurement vector. The Kalman filter algorithm is commonly used to estimate the state and error covariance of the system from the measurements. The equations for the Kalman filter are outlined as follows.

Time Update:

$$X_{k|k-1} = F_{k-1}X_{k-1|k-1} \tag{2.3}$$
$$P_{k|k-1} = F_{k-1}P_{k-1|k-1}F_{k-1}^T + G_{k-1}Q_{k-1}G_{k-1}^T \tag{2.4}$$

Measurement Update:

$$X_{k|k} = X_{k|k-1} + K_k[Z_k - H_kX_{k|k-1}] \tag{2.5}$$
$$P_{k|k} = [I - K_kH_k]P_{k|k-1} \tag{2.6}$$
$$K_k = P_{k|k-1}H_k^T[H_kP_{k|k-1}H_k^T + R_k]^{-1} \tag{2.7}$$

where $X_{i|j}$ denotes the state estimate for time i given measurements through time j, and $P_{i|j}$ denotes the corresponding error covariance.

2.1 Kinematic Constraint for Constant Speed Targets

A kinematic constraint can be utilized as additional information about the target motion to reduce the errors in the estimates due to the time-varying accelerations. Using the kinematic constraint tends to force the acceleration estimates to change in a manner that is consistent with the dynamics of the target. A kinematic constraint can be developed for use in tracking constant speed, maneuvering targets. The speed of a target is given by

$$S = (\dot{x}^2 + \dot{y}^2 + \dot{z}^2)^{\frac{1}{2}} \tag{2.8}$$

For a target moving at a constant speed,

$$\frac{dS}{dt} = 0 \qquad \text{or} \qquad (\dot{x}\ddot{x} + \dot{y}\ddot{y} + \dot{z}\ddot{z}) = V \cdot A = 0 \tag{2.9}$$

where V and A are the target velocity and acceleration vectors, respectively.

This kinematic constraint for constant speed targets is useful information and can be incorporated in the system state, Eq. (2.1), or used as a pseudomeasurement in conjunction with Eq. (2.2). While both approaches are conceptually feasible, the second approach is more attractive because the first changes the state equation from linear to nonlinear. In the implementation of the extended Kalman filter, including nonlinearities in the measurement equation are computationally less expensive than in the state equation [7]. Thus, the kinematic constraint in Eq. (2.9) is incorporated into the filter through a pseudomeasurement as discussed in [5]. The pseudomeasurement equation is given by

$$\frac{V_{k|k}}{S_{k|k}} \cdot A_k + \mu_k = 0 \tag{2.10}$$

where

$$V_{k|k} = [\,\dot{x}_{k|k} \quad \dot{y}_{k|k} \quad \dot{z}_{k|k}\,] \qquad S = (\dot{x}^2_{k|k} + \dot{y}^2_{k|k} + \dot{z}^2_{k|k})^{\frac{1}{2}} \tag{2.11}$$

and $\mu_k \sim N(0, R^\mu_k)$. The μ_k is a white Gaussian error process that accounts for the uncertainty in both $V_{k|k}$ and the constraint. Since the initial estimates of $V_{k|k}$ may be very poor, R^μ_k is initialized with a large value and allowed to decrease as

$$R^\mu_k = r_1(\delta)^k + r_0 \tag{2.12}$$

where $0 < \delta < 1$, r_1 is a constant chosen large for initialization, and r_0 is a constant chosen for steady-state conditions.

The filtering equations for this formulation of the kinematic constraint are given in the following equations with $X^c_{k|k}$ denoting the state estimate after the constraint has been applied, and $P^c_{k|k}$ denoting the associated state error covariance. The filtering equations are

$$X_{k+1|k} = F_k X^c_{k|k} \qquad P_{k|k-1} = F_{k-1}P^c_{k-1|k-1}F^T_{k-1} + G_{k-1}Q_{k-1}G^T_{k-1} \tag{2.13}$$

$$X_{k|k} = X_{k|k-1} + K_k[Z_k - H_k X_{k|k-1}] \qquad P_{k|k} = [I - K_k H_k]P_{k|k-1} \tag{2.14}$$

$$X^c_{k|k} = [I - K^c_k C_k]X_{k|k} \qquad P^c_{k|k} = [I - K^c_k C_k]P_{k|k} \tag{2.15}$$

where

$$K_k = P_{k|k-1}H^T_k[H_k P_{k|k-1}H^T_k + R_k]^{-1} \tag{2.16}$$

$$K^c_k = P_{k|k}C^T_k[C_k P_{k|k}C^T_k + R^\mu_k]^{-1} \tag{2.17}$$

$$C_k = \frac{1}{S_{k|k}}[0 \quad 0 \quad \dot{x}_{k|k} \quad 0 \quad 0 \quad \dot{y}_{k|k} \quad 0 \quad 0 \quad \dot{z}_{k|k}\,] \tag{2.18}$$

Simulation results that demonstate the benefits of using the kinematic constraint are given in [5,8] along with discussion concerning the biasness and stability of a filter using the kinematic constraint as a pseudomeasurement.

2.2 Exponentially Increasing Acceleration (EIA) Model

The EIA model is derived from the exponentially-correlated acceleration model introduced in [9] where the negative correlation coefficient is replaced by a positive coefficient. Thus, the state model will have a pole outside the unit circle. The discrete-time EIA model is given by Eq. (2.1) for a single coordinate with

$$F_k = \begin{bmatrix} 1 & T & \tau^{-2}(e^{\tau T} - \tau T - 1) \\ 0 & 1 & \tau^{-1}(e^{\tau T} - 1) \\ 0 & 0 & e^{\tau T} \end{bmatrix} \qquad G_k = \begin{bmatrix} \tau^{-3}(e^{\tau T} - 1 - \tau T - 0.5(\tau T)^2) \\ \tau^{-2}(e^{\tau T} - 1 - \tau T) \\ \tau^{-1}(e^{\tau T} - 1) \end{bmatrix} \tag{2.19}$$

and τ defining the correlation time constant for the acceleration. The elements of the state vector X_k are position, velocity, and acceleration. Since the (3,3) element of F_k is greater than one, the magnitude of the acceleration in each coordinate will increase during the prediction from time k to time $k+1$. This model can be used in a multiple model algorithm because other models are available to ensure stability. In fact, when used in the IMM algorithm, the probability of the EIA model remains very low except at the beginning of a maneuver. Simulation results that demonstate the use of this model in the IMM algorithm are given in Section 3.

2.3 Turning Rate Estimator (TRE) Model

The TRE model as presented in [6] is a nonlinear state model that includes position, velocities, and a turning rate in the state. The discrete-time update of the state is given by

$$X_{k+1} = f(X_k) = \begin{bmatrix} x_k + T\dot{x}_k - 0.5T^2\dot{y}_k\omega_k \\ (1 - 0.5T^2\omega_k^2)\dot{x}_k - T\dot{y}_k\omega_k \\ y_k + T\dot{y}_k + 0.5T^2\dot{x}_k\omega_k \\ (1 - 0.5T^2\omega_k^2)\dot{y}_k + T\dot{x}_k\omega_k \\ z_k + T\dot{z}_k \\ \dot{z}_k \\ \omega_k \end{bmatrix} \tag{2.20}$$

The time update of the state error covariance is given by Eq. (2.4), where

$$F_k = \left.\frac{\partial f(X_k)}{\partial X_k}\right|_{X_k = X_{k|k}} \tag{2.21}$$

$$G_k Q_k G_k^T = q_k \begin{bmatrix} B_k & 0_{2\times2} & 0_{2\times2} & 0_{2\times1} \\ 0_{2\times2} & B_k & 0_{2\times2} & 0_{2\times1} \\ 0_{2\times2} & 0_{2\times2} & B_k & 0_{2\times1} \\ 0_{1\times2} & 0_{1\times2} & 0_{1\times2} & \dfrac{\sigma_\omega^2 T^2}{q_k} \end{bmatrix} \quad \text{with} \quad B_k = \begin{bmatrix} 0.25T^4 & 0.5T^3 \\ 0.5T^3 & T^2 \end{bmatrix} \tag{2.22}$$

q_k is a scalar acceleration variance, and σ_ω^2 is the variance of the turning rate error. Note that the process noise covariance has been modified from that in [6] by adding uncertainty to the velocity estimates. Simulation studies showed that the use of the process noise covariance in [6] resulted in volatile position estimates. Furthermore, the process noise covariance in Eq. (2.22) includes a dependence on the sample period so that various data rates can be handled readily. From Eq. (2.20), it is obvious that the maneuver is confined to the horizontal plane, which a significant limitation of this model.

2.4 The IMM Algorithm

An important problem in state estimation is the estimation of the state of a linear system with Markovian switching coefficients. In this problem, the dynamics of the system are represented by multiple models which are hypothesed to be correct. Efficient management of the multiple hypotheses is critical to limiting the computational requirements while maintaining the performance capability of the algorithm. The IMM algorithm is a novel approach to merging the different model hypotheses [1,2]. Furthermore, previous investigations in the literature indicate that the IMM algorithm is the superior technique when the computational requirements of the different techniques are considered [2,3,4]. Such a linear system with Markovian switching coefficients can be represented as

$$X_{k+1} = F_k(\theta_k)X_k + G_k(\theta_k)w_k \tag{2.23}$$

$$Y_k = H_k(\theta_k)X_k + v_k \tag{2.24}$$

where X_k is the system state, and θ_k is a finite state Markov chain taking values in $\{1, ..., N\}$ according to the probability p_{ij} of transitioning from model i to model j. The w_k and v_k are white Gaussian errors for the system state and measurement processes.

The IMM algorithm consists of a filter for each model, a model probability evaluator, an estimate mixer at the input of the filters, and an estimate combiner at the output of the filters. The multiple models interact

through the mixing to track a target maneuvering through an arbitrary trajectory. The flow diagram of an IMM filter with two models is given in Figure 1, where $X(k|k)$ is the state estimate based on both models, $X^j(k|k)$ is the state estimate for time k based on model j, $\Lambda(k)$ is the vector of model likelihoods at time k, and $\mu(k)$ is the vector of model probabilities at time k when all the likelihoods have been considered. With the assumption that the model switching is governed by an underlying Markov chain, the mixer uses the model probabilities and the model switching probabilities to compute a mixed estimate for each filter. At the beginning of a filtering cycle, each filter uses a mixed estimate and a measurement to compute a new estimate and a likelihood for the model within the filter. The likelihoods, prior model probabilities, and the model switching probabilities are then used to compute new model probabilities. The overall state estimate is then computed with the new state estimates and their model probabilities. For space considerations, subscripts will be used to denote time throughout the paper (i.e. $\mu_k(j)$ is the probability that model j is correct at time k). The IMM algorithm for tracking with N models is outlined in the following 5 steps. A derivation and detailed explanation of the IMM algorithm are given in [2,4].

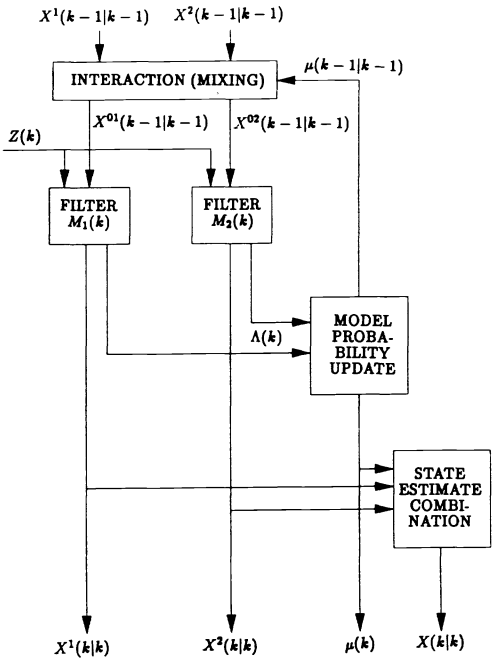

Figure 1. The IMM Algorithm

Step 1: Mixing of State Estimates

The filtering process starts with *a priori* state estimates $X^j_{k-1|k-1}$, state error covariances $P^j_{k-1|k-1}$, and the associated probabilities $\mu_{k-1}(j)$ for each model. The mixed state estimate for model j at time k, $M_k(j)$, is computed as

$$X^{0j}_{k-1|k-1} = \sum_{i=1}^{N} X^i_{k-1|k-1}\mu_{k-1|k-1}(i|j) \tag{2.25}$$

where

$$\mu_{k-1|k-1}(i|j) = \frac{1}{\bar{c}_j}p_{ij}\mu_{k-1}(i) \qquad \bar{c}_j = \sum_{i=1}^{N} p_{ij}\mu_{k-1}(i) \tag{2.26}$$

and p_{ij} is the assumed transition probability for switching from model i to model j, and $\bar{c}_j$ is a normalization constant. The mixed state error covariance for $M_k(j)$ is computed as

$$P^{0j}_{k-1|k-1} = \sum_{i=1}^{N}[P^i_{k-1|k-1} + (X^i_{k-1|k-1} - X^{0j}_{k-1|k-1})(X^i_{k-1|k-1} - X^{0j}_{k-1|k-1})^T]\mu_{k-1|k-1}(i|j) \tag{2.27}$$

Step 2: Model Updates

The Kalman filtering equations provide the model updates. When the kinematic constraint is implemented in the IMM algorithm, it is applied as in Eq. (2.15) after the mixing and after the measurement update. The constraint is applied after the mixing so that its effect will be reflected in the residuals. It is also applied after the measurement update so that its effect is reflected in the filter output.

Step 3: Model Likelihood Computations

The likelihood of $M_k(j)$ is computed with the filter residuals $\tilde{Z}^j_k$, the covariance of the filter residuals T^j_k, and the assumption of Gaussian statistics. The likelihood of $M_k(j)$ is given by

$$\Lambda^j_k = \frac{1}{\sqrt{|2\pi T^j_k|}}\exp[-0.5(\tilde{Z}^j_k)^T(T^j_k)^{-1}\tilde{Z}^j_k] \tag{2.28}$$

Step 4: Model Probabilities Update

The model probabilities are updated as

$$\mu_k(j) = \frac{1}{c}\Lambda_k(j)\bar{c}_j \qquad \text{where} \qquad c = \sum_{i=1}^{N}\Lambda_k(i)\bar{c}_i \tag{2.29}$$

Step 5: Combination of State Estimates

The state estimate and error covariance for the IMM algorithm output are obtained from a probabilistic sum of the individual filter outputs and given by

$$X_{k|k} = \sum_{i=1}^{N} X^i_{k|k}\mu_k(i) \qquad P_{k|k} = \sum_{i=1}^{N}\mu_k(i)[P^i_{k|k} + (X^i_{k|k} - X_{k|k})(X^i_{k|k} - X_{k|k})^T] \tag{2.30}$$

3. Proposed IMM Algorithm

The IMM algorithm proposed for tracking targets that maneuver through coordinated turns includes a CV model, an EIA model, and a 3DTRKC model. This IMM algorithm will be referred as CVEIA3DTRKC. The CV model provides good tracking when the target is not maneuvering, while the 3DTRKC model provides tracking through the maneuver, and the EIA model provides maneuver response. When the kinematic constraint is implemented in the IMM algorithm, it is applied as in Eq. (2.15) after the mixing and after the measurement update. Some results that demonstrate the benefits of the EIA model, the kinematic constraint, and the 3DTRKC model are presented in this section.

The 3DTR model is a nonlinear state model in that the velocity and acceleration estimates are used to compute the turning rate that is used as a parameter in the state transition matrix. The state includes position, velocities, and accelerations. The discrete-time update of the filter is given by Eqs. (2.3) and (2.4) where

$$F_k = \begin{bmatrix} A_k & 0_{3\times3} & 0_{3\times3} \\ 0_{3\times3} & A_k & 0_{3\times3} \\ 0_{3\times3} & 0_{3\times3} & A_k \end{bmatrix} \qquad \text{with} \qquad A_k = \begin{bmatrix} 1 & \omega_k^{-1}\sin(\omega_k T) & \omega_k^{-2}(1-\cos(\omega_k T)) \\ 0 & \cos(\omega_k T) & \omega_k^{-1}\sin(\omega_k T) \\ 0 & -\omega_k\sin(\omega_k T) & \cos(\omega_k T) \end{bmatrix} \tag{3.1}$$

and the process noise covariance is that of the constant acceleration model. The turning rate, ω_k, is calculated from state estimates and is the magnitude of the acceleration divided by the speed of the target.

For this simulation study, the radar tracking system has measurements that are zero-mean Gaussian with standard deviations of 8 meters in range and 0.002 radians in bearing and elevation. The radar measures the target position at 4 Hz. The target trajectory to be considered has an initial position of $(12.3, 9.5, 0.2)$ km and initial velocity of $(-320, -85, 0)$ m/s. The target moves with constant velocity from 0 to 7 seconds, from 15 to 22 seconds, and from 30 to 39 seconds. The target performs two 5 g, constant speed maneuvers from 7 to 15 seconds and from 22 to 30 seconds. A second order, criticaly-damped system with natural frequency of 2 rad/sec was used to model the target response to acceleration commands. All simulation results were obtained through Monte Carlo simulations with 100 experients.

The benefits of the EIA model will be addressed first by considering the CVEIACA algorithm which includes (1) a CV model, (2) an EIA model, and (3) a CA model. For the CVEIACA, the process noise covariances are $Q^1_k = 0.01\ I_3 \text{m}^2/\text{s}^4$, $Q^2_k = 484\ I_3\ \text{m}^2/\text{s}^6$, and $Q^3_k = 50.4\ I_3\ \text{m}^2/\text{s}^6$, where I_3 is 3×3 idenity matrix. For the EIA model, $\tau = 0.89$ Hz. The CV2CA algorithm, which is a common model configuration for the IMM algorithm, will be used as a basis for evaluating the benefits of the EIA model. The CV2CA algorithm includes (1) a CV model, (2) a CA model for maneuver response, and (3) a CA model for tracking through the maneuver. For the CV2CA, the process noise covariances are $Q^1_k = 0.01\ I_3 \text{m}^2/\text{s}^4$, $Q^2_k = 441\ I_3\ \text{m}^2/\text{s}^6$, and $Q^3_k = 50.4\ I_3\ \text{m}^2/\text{s}^6$. Both algorithms have the same initial model probabilities $\mu_0 = [0.9 \quad 0 \quad 0.1]$ and the model switching probabilities are

$$\Pi(\text{CVEIACA}) = \begin{bmatrix} 0.98 & 0.02 & 0 \\ 0 & 0.7 & 0.3 \\ 0.05 & 0 & 0.95 \end{bmatrix} \qquad \Pi(\text{CV2CA}) = \begin{bmatrix} 0.95 & 0.05 & 0 \\ 0 & 0.7 & 0.3 \\ 0.08 & 0 & 0.92 \end{bmatrix} \tag{3.2}$$

The Root-Mean-Square Errors (RMSE) of the two algorithms are given in Figure 2. The average model probabilities for both IMM algorithms are given in the first two plots in Figure 3, where IMM3 is used to denote the IMM algorithm with three models. The use of the EIA model has reduced the amount of error incurred at the beginning of the maneuver. This reduction in acceleration error allows the filter used for tracking through the maneuver to respond earlier to provide improved tracking performance during this portion of a maneuver. The model probability of the EIA increases slightly at the beginning of the maneuver to provide this improved performance, as shown in the second plot of Figure 3.

The benefits of the kinematic constraint will be considered next with the CVEIACAKC algorithm which includes (1) a CV model, (2) an EIA model, and (3) a CA model with the kinematic constraint. For the CVEIACAKC, the process noise covariances, initial model probabilities, and model switching probabilities were not changed from the CVEIACA. The constraint variance is given by $(500(0.9)^k + 32)$ m^2/s^4. The RMSE of the CVEIACA and CVEIACAKC are given in Figure 4. The average model probabilities for the CVEIACAKC are given in the third plot in Figure 3. During the maneuver, there is uncertainty in whether the CV or CA model of the CVEIACA should be used. The use of the kinematic constraint with the CA model has eliminated this probelm as shown in the model probabilities for the CVEIACAKC. Notice the improved performance for the CVEIACAKC when tracking the target during the maneuver.

Finally, the benefits of the 3DTR model will be considered with the CVEIA3DTRKC algorithm which includes (1) a CV model, (2) an EIA model, and (3) a 3DTRKC model. For the CVEIA3DTRKC, the process noise covariance for the 3DTR is $Q_k^3 = 100\ I_3$ m^2/s^6, and the constraint variance is given by $(500(0.9)^k + 16)$ m^2/s^4. The remaining process noise covariances are the same as for the CVEIACA. The model switching probabilities are

$$\Pi(\text{CVEIA3DTRKC}) = \begin{bmatrix} 0.98 & 0.02 & 0 \\ 0 & 0.7 & 0.3 \\ 0.04 & 0 & 0.96 \end{bmatrix} \tag{3.3}$$

The RMSE of the two algorithms are given in Figure 5. A reduction in the tracking error has come about by including the EIA model for maneuver response and the kinematic constraint for tracking during the maneuver. By replacing the CAKC model with the 3DTRKC model for tracking during the maneuver, increased tracking accuracy can be realized. The 3DTRKC model is designed to track targets through coordinated turns and, as a result, provides better tracking than the CAKC model.

4. Simulation Results for Comparison IMM Algorithms

The IMM algorithm proposed in [6] for tracking maneuvering targets includes a CV model and a TRE model and is denoted as CVTRE. The target trajectory presented in Section 3 is used to compare the CVTRE and CVEIA3DTRKC algorithms. The CVEIA3DTRKC algorithm will use the parameters given in Section 3. For the CVTRE, the process noise covariance for the CV model is $Q_k^1 = 1\ I_3$ m^2/s^4, and for the TRE model is $q_k^3 = 100$ m^2/s^4 and $\sigma_\omega^2 = 0.01$ rad^2/s^4. The initial model probabilities are $\mu_0 = [0.95 \quad 0.05]$ and the model switching probabilities are

$$\Pi(CVTRE) = \begin{bmatrix} 0.95 & 0.05 \\ 0.05 & 0.95 \end{bmatrix} \tag{4.1}$$

The RMSE of the two algorithms are given in Figure 6 with the model probabilities given in Figure 7. The tracking accuracy for the two configurations is very similar, with the CVTRE slightly better than the CVEIA3DTRKC. However, the CVTRE does not provide estimates of the acceleration, which is a difficult parameter to estimate. The magnitude of the turning rate is also shown in Figure 6. The CVTRE directly estimates the turning rate as a state parameter, while the CVEIA3DTRKC uses state estimates to calculate the turning rate. Nonetheless, both models estimate the magnitude of the turning rate with similar performance. The CVTRE does not have a transition model like the CVEIA3DTRKC and this point is reflected in the model probabilites.

For comparing the two IMM algorithms, the previous trajectory was rotated 5° about the x and y axes before tracking. The RMSE of the two algorithms are given in Figure 8 with the model probabilities given in Figure 9. Since the CVTRE is designed to track in the horizontal plane, any deviation from this plane results in large tracking errors. A comparison shows CVEIA3DTRKC provides better tracking throughout the entire maneuver. Its model probabilities are very similar to the ones for the target maneuvering in the horizontal plane. The CVTRE is very uncertain when the maneuver has ended as shown in its model probabilities. Slight deviations from the horizontal plane yield unacceptable tracking results when using the CVTRE.

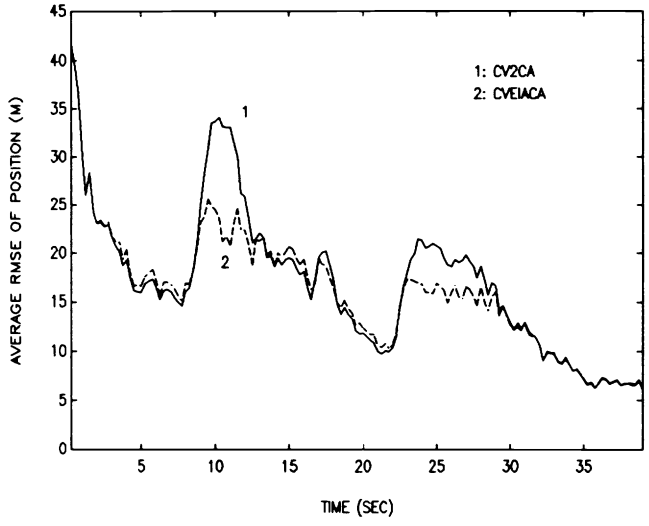

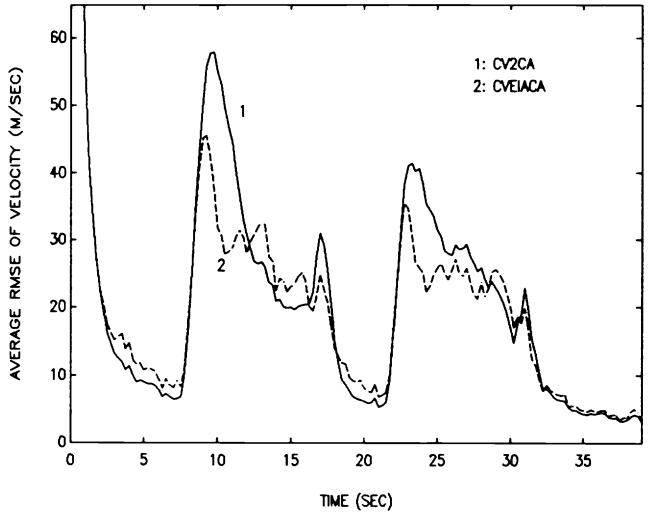

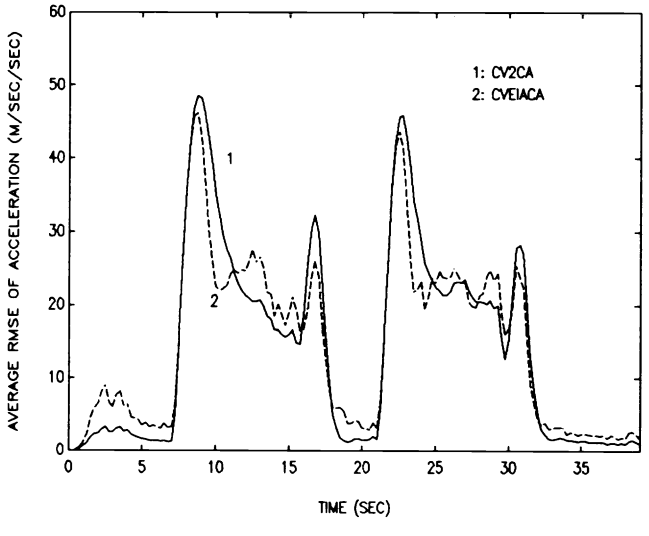

Fig. 2. RMS Errors for Case 1

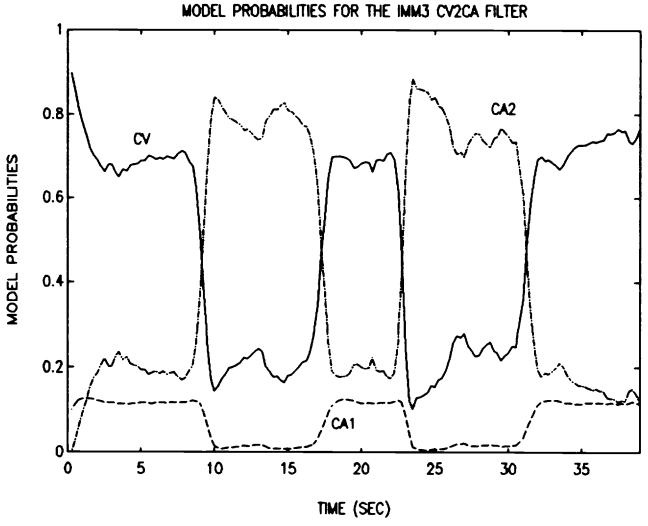

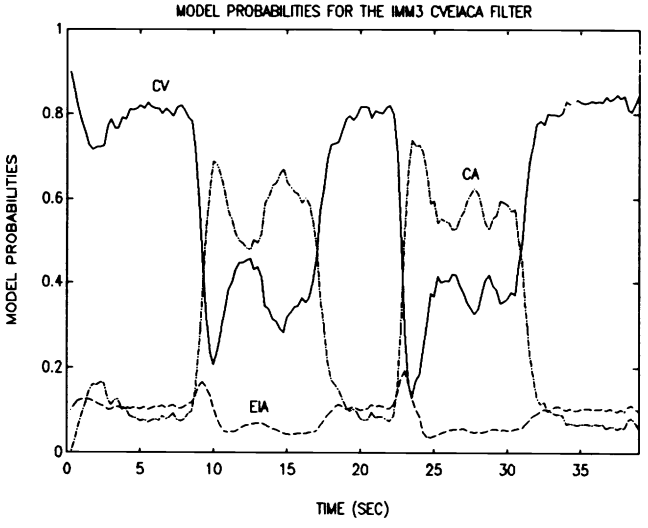

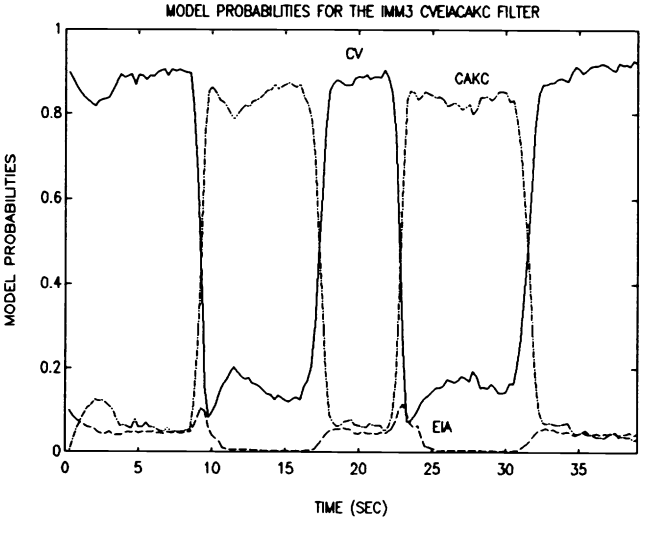

Fig. 3. Model Probabilities for Cases 1 and 2

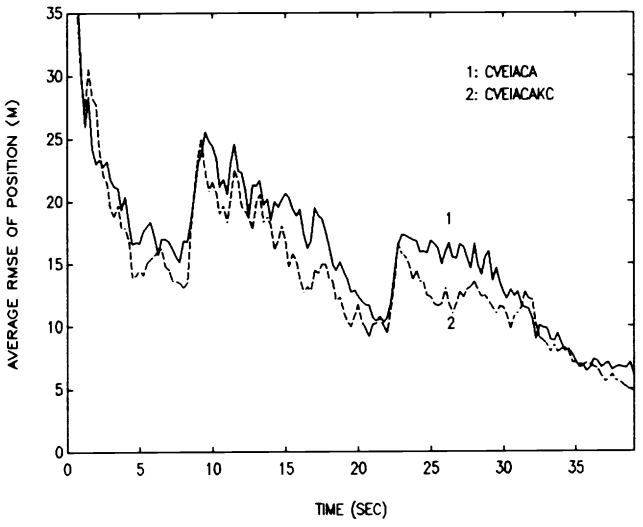

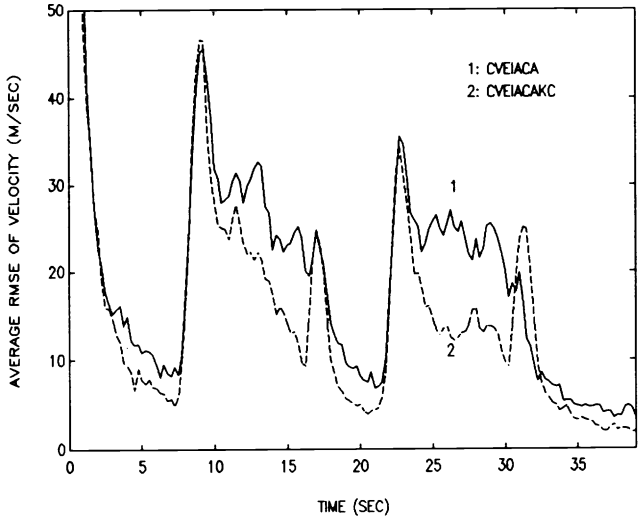

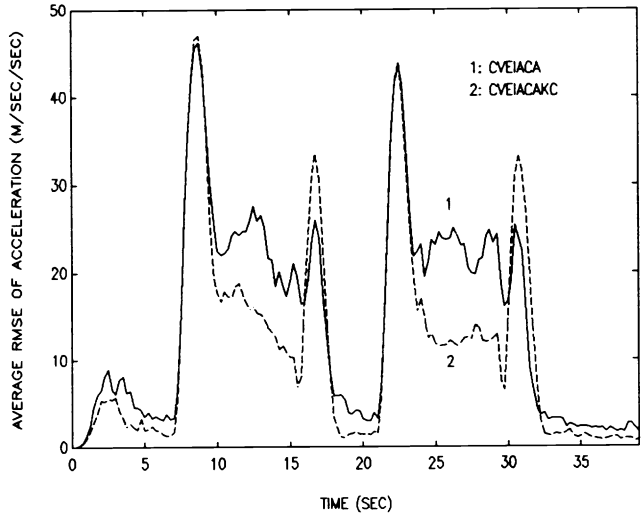

Fig. 4. RMS Errors for Case 2

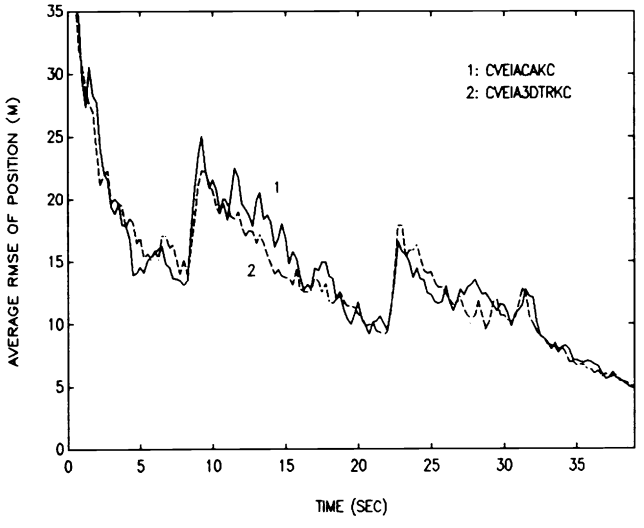

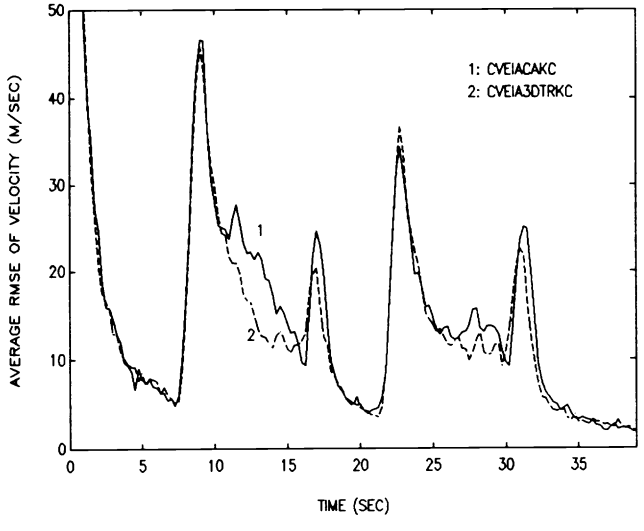

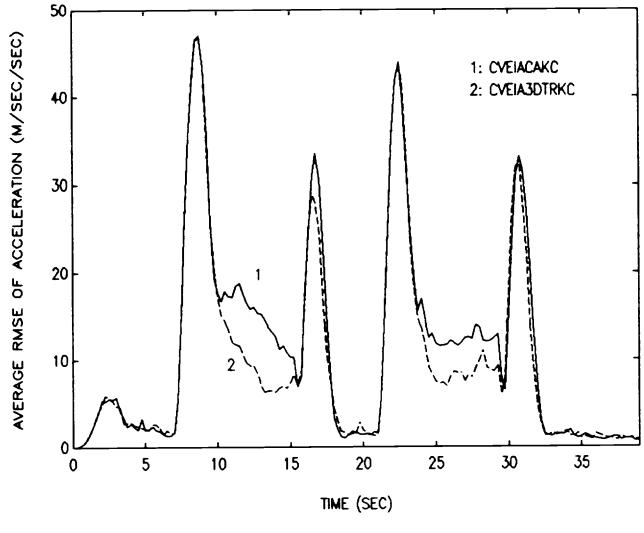

Fig. 5. RMS Errors for Case 3

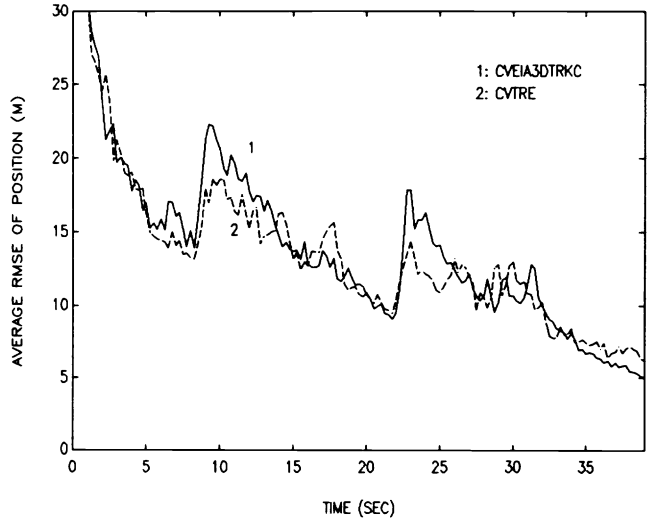

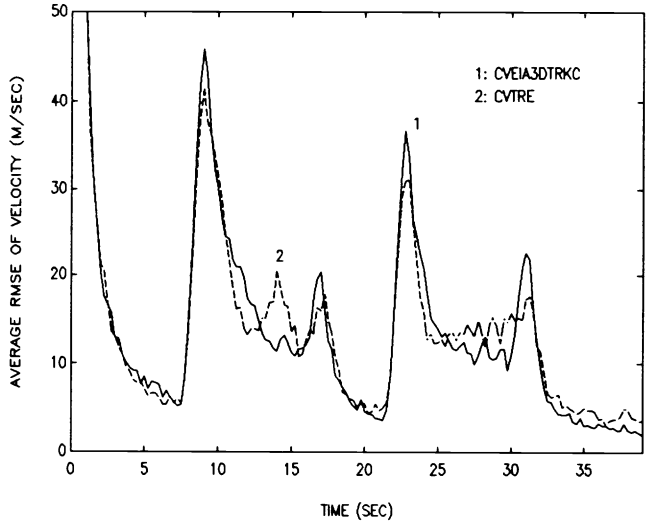

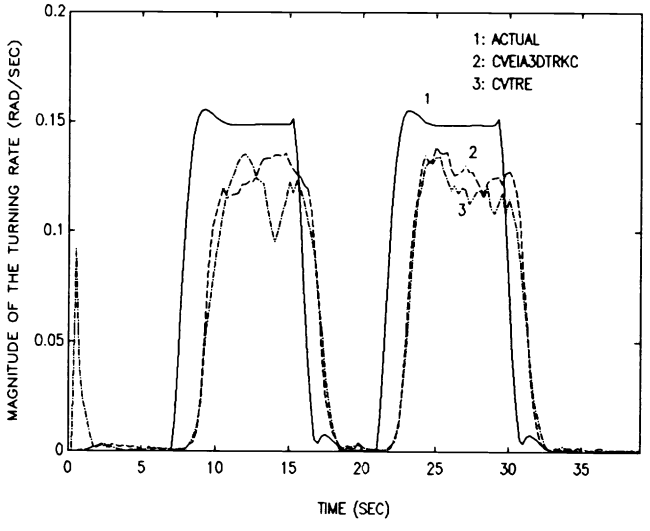

Fig. 6. RMS Errors for Case 4

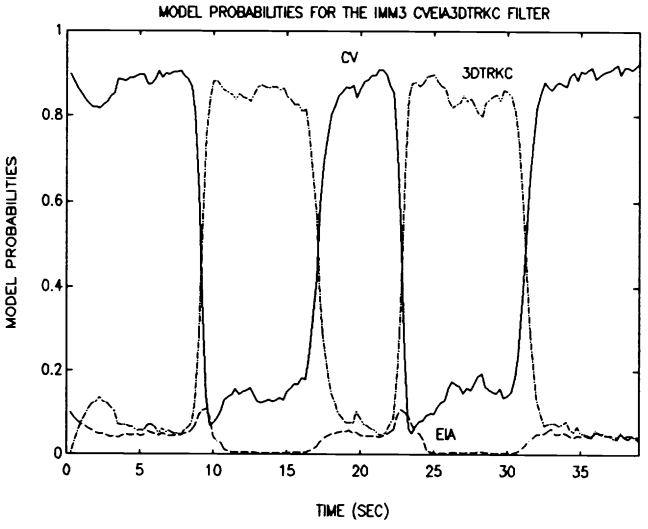

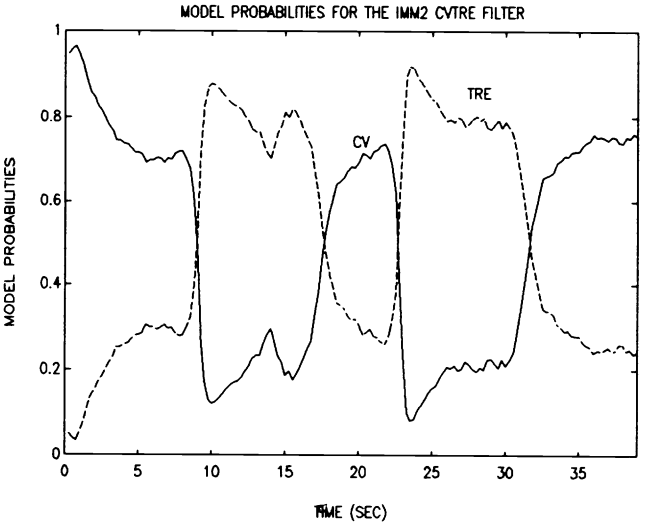

Fig. 7. Model Probabilities for Case 4

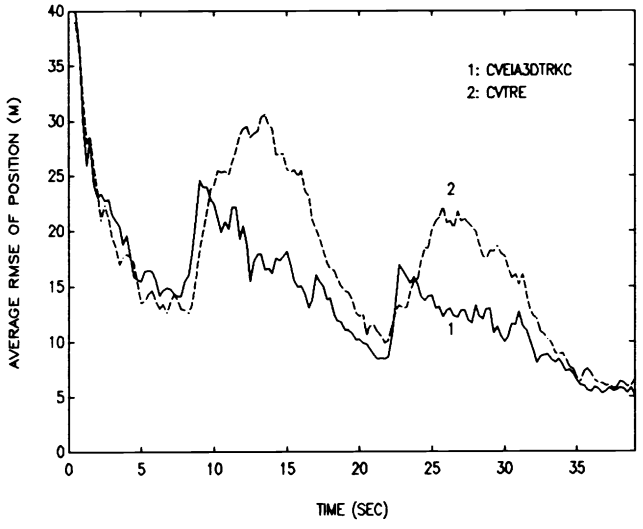

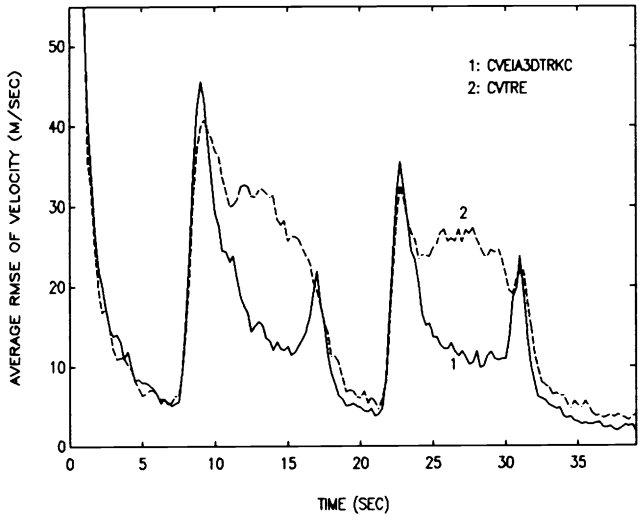

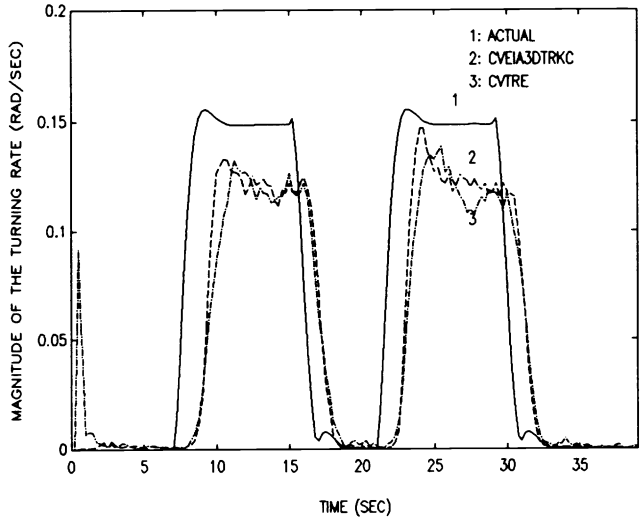

Fig. 8. RMS Errors for Case 5

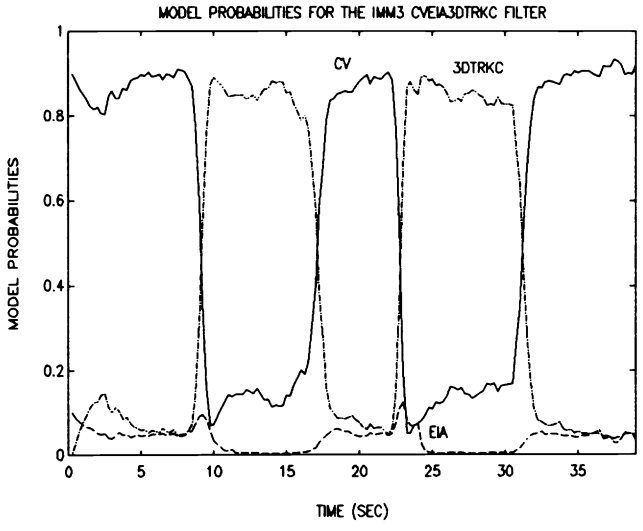

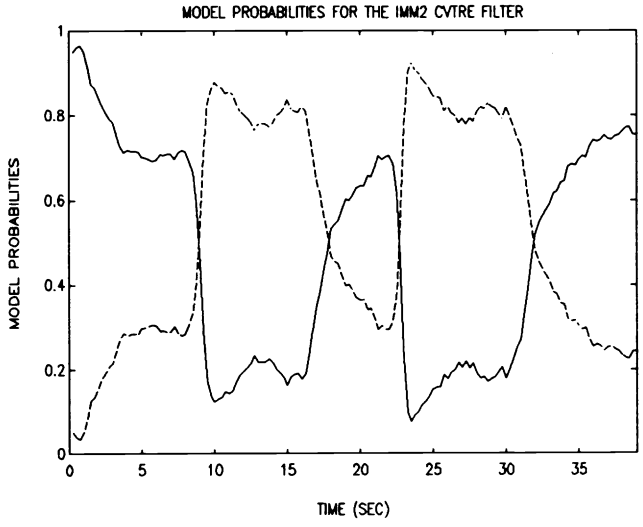

Fig. 9. Model Probabilities for Case 5

5. Summary and Conclusions

The benefits of using the EIA and 3DTR models, and the kinematic constraint for constant speed targets in the IMM configuration has been clearly demonstrated. The inclusion of the EIA model instead of a CA model for maneuver response greatly reduced the lag in the acceleration estimates for the initial portion of a maneuver. The kinematic constraint for constant speed targets is a valuable asset for tracking targets making coordinated turns. Applying the kinematic constraint in the mannner proposed provides improved the estimates for both mixing and output as well as reducing the model uncertainty. Further improvement in the maneuvering phase must come from choosing models better suited for this task. The CA model can be used for the maneuvering phase of the trajectory. However, this model is not well suited for coordinated turns because it does not maintain the constant speed characteristic of the target. Unlike the CA model, the 3DTR model maintains this characteristic. Therefore, its use is well suited for such maneuvers as demonstrated by the simulation results. The use of the 3DTR model instead of the CA model provided improved tracker accuracy by using the inherent turning rate information stored in the state estimates.

The 3DTR model is not confined to a arbitrary plane like the TRE model. The tracking performance for the CVTRE is slighly better than the CVEIA3DTRKC when the target was maneuvering in the horizontal plane. However, when the target was tilted 5^o about the x and y axes, the performance of the CVTRE degraded substantially, while the CVEIA3DTRKC performance remained relatively constant. The drawbacks of the CVTRE is that it does not estimate the accelerations of the target and maneuvers are confined to a plane. The CVTRE is computationally less expensive than the CVEIA3DTRKC, but it cannot overcome its drawbacks. The CVEIA3DTRKC model is very effective in tracking maneuvering targets because it provides improved maneuver response and reduced tracking errors in the maneuvering phase while estimating the accelerations of target.

The authors are currently involved in the development of the Interacting Multiple Acceleration Model (IMAM) algorithm to reduce the computational cost of implementing the IMM algorithm. In the IMAM algorithm, multiple acceleration models are driven with one constant velocity model to reduce the computational cost significantly.

Acknowledgements

This work was support by the NSWCDD Independent Exploratory Development Program, Naval Surface Warfare Center, Dahlgren Division, Dahlgren, Virginia.

References

1. Blom, H.A.P., "An Efficient Filter for Abruptly Changing Systems," Proc. 23^{rd} Conf. on Decision and Control, Las Vegas, NV, 1984, pp. 656-658.
2. Blom, H.A.P., and Y. Bar-Shalom, "The Interacting Multiple Model Algorithm for Systems with Markovian Switching Coefficients," *IEEE Trans. Auto. Cont.*, 1988, pp. 780-783.
3. Tugniat, J.K., "Detection and Estimation for Abruptly Changing Systems," *Automatica*, 1982, pp. 607-615.
4. Bar-Shalom, Y., C.Y. Chang, and H.A.P. Blom, "Tracking a Maneuvering Target Using Input Estimation Versus The Interacting Multiple Model Algorithm," *IEEE Trans. Aero. Elect. Syst.*, 1989, pp. 296-300.
5. Alouani, A.T., and W.D. Blair, "Use of Kinematic Constraint in Tracking Constant Speed, Tracking Maneuvering Targets," *Proc. of 30^{th} IEEE Conf. on Dec. and Cont.*, Brighton, UK, Dec. 1991, 2059-2062.
6. Dufour, F., and M. Mariton, "Tracking a 3D Maneuvering Target with Passive Sensors," *IEEE Trans. Aero. and Elect. Sys.*, 1991, pp. 725-739.
7. Tahk, M., and J.L. Speyer, "Target Tracking Problems Subject to Kinematic Constraints," *IEEE Trans. Auto. Cont.*, 1990, pp. 324-326.
8. W.D. Blair, G.A. Watson, and A.T. Alouani, *Use of Kinematic Constraint in Tracking Constant Speed, Tracking Maneuvering Targets*, Technical Report NAVSWC TR 91-561, Naval Surface Warfare Center, Dahlgren VA, Nov. 1991.
9. Singer, R.A., "Estimation of Optimal Tracking Filter Performance for Manned Maneuvering Targets," *IEEE Trans. Aero. and Elect. Sys.*, 1970, pp. 473-483.